STAR-eX: A Student-Teacher Assistive Rehabilitation Exoskeleton for Post-Stroke Mirror Therapy Hand Hemiplegia

Afonso Araújo[1], Athanasios Vourvopoulos[2] and Alexandre Bernardino[1]

***Abstract*— Traditional Mirror Therapy (MT) uses the reflection of an unaffected limb to promote neural recovery in the affected limb post-stroke. Robotic Mirror Therapy (RMT) has since emerged with robotics development, but current devices are often unsuitable for Point-of-Care (POC) due to their cost, complexity, and lack of user-friendliness. To address these issues, we developed a portable, affordable, and user-friendly hand-finger rehabilitation system integrating a 21-Degree-of-Freedom (DoF) parallel manipulator (5 active DoF), a motion sensor, and a Virtual Reality (VR) piano task. The VR tasks, inspired by RMT, Robotic Therapy (RT), and MT, leverage Discrete Sequence Progress Tasks (DSPTs) to engage brain regions responsible for sequential actions, critical for Activities of Daily Living (ADL). Operating in a student-teacher configuration, the system mirrors movements of the unaffected hand onto the affected hand, forming a neurological loop. Tested with 16 participants, our system demonstrated superior motor skill acquisition compared to RT.**

***Index Terms*— Discrete Sequence Progress Tasks; Exoskeleton; Robotic Mirror Therapy; Stroke Rehabilitation; Virtual Reality.**

I. INTRODUCTION

Stroke remains a leading cause of death globally, with 1.12 million new cases recorded in Europe in 2017. This figure is projected to rise by 3% by 2047, while the number of stroke survivors is expected to increase by 27%, reaching 12.11 million [1]. Although mortality rates dropped by 18% from 2010 to 2019, stroke continues to be the primary cause of long-term disability, generating healthcare costs of 45€ billion annually [1]. Traditional rehabilitation methods, such as the Bobath Method and Constraint-Induced Movement Therapy (CIMT), are commonly employed to promote motor recovery. However, these techniques often foster compensatory strategies rather than genuine motor rehabilitation, limiting functional gains [2]. Distal limb rehabilitation poses particular challenges, as fine motor control is crucial and recovery is complicated by the increased neural distance from the brain [3].

To overcome these challenges, Discrete Sequence Progress Tasks (DSPTs) have emerged as an effective method to reinforce motor learning. DSPTs involve structured movement sequences, such as key presses, activating pre-planning and real-time execution mechanisms [4]. This structured repetition helps patients develop fine motor skills vital for Activities of Daily Living (ADL), including buttoning shirts and tying shoelaces.

The integration of Virtual Reality (VR) into DSPT environments enhances immersion and engagement, facilitating greater motivation and gamifying the rehabilitation process. VR systems provide repetitive, intensive exercises essential for neuroplasticity while offering real-time feedback. Rehabilitation Gaming Systems (RGS) leverage VR to create task-oriented exercises that engage stroke-affected neural pathways, dynamically adjusting difficulty in response to patient performance to promote skill transfer to real-life activities [5]. The use of mirror neuron principles, where patients observe virtual limbs reflecting their actions, further enhances motor outcomes [6].

Robotic Mirror Therapy (RMT) combines VR and robotic systems to synchronize limb movements and promote neuroplasticity and motor recovery [7]. However, existing RMT devices are often costly and confined to clinical environments, limiting their accessibility for point-of-care (POC) treatment. Devices such as the ARMin V [9] and Lokomat, priced at around $235,000 [1], exemplify the financial and logistical barriers preventing widespread adoption, especially in home-based rehabilitation.

To address these limitations, the STAR-eX (Student-Teacher Assistive Rehabilitation Exoskeleton) was developed to facilitate fine finger movement rehabilitation in stroke patients. The STAR-eX employs a student-teacher configuration, where a motion sensor tracking the healthy hand guides the unhealthy hand via an exoskeleton, whilst interacting with VR piano-playing tasks. This design emphasizes bilateral training and ADL-focused exercises, fostering improved distal limb recovery. The STAR-eX prioritizes affordability, portability, and user-friendliness, offering a practical alternative to conventional rehabilitation systems.

II. BACKGROUND

Student-teacher systems have emerged as a key focus in rehabilitation technology due to their ability to enable real-time control and replicate movement patterns accurately. These systems typically consist of a teacher device controlled by the patient's healthy limb and a student device that

*This work was supported by the Portuguese Foundation for Science and Technology (FCT) through LARSyS - FCT (DOI: 10.54499/LA/P/0083/2020, 10.54499/UIDP/50009/2020, and 10.54499/UIDB/50009/2020), and the NOISyS project (DOI: 10.54499/2022.02283.PTDC).

[1]Department of Electrical and Computer Engineering, Institute for Systems and Robotics (ISR-Lisboa), Instituto Superior Técnico, Lisbon, Portugal. afonso.d.araujo@tecnico.ulisboa.pt alexandre.bernardino@tecnico.ulisboa.pt

[2]Department of Bioengineering, Institute for Systems and Robotics (ISR-Lisboa), Instituto Superior Técnico, Lisbon, Portugal. athanasios.vourvopoulos@tecnico.ulisboa.pt

[1]https://www.umms.org/rehab/health-services/therapeutic-technology/lokomat-therapy

mirrors the movements on the impaired limb, providing active, coordinated assistance.

While each system offers a unique approach to building a student-teacher rehabilitation device, systems that have undergone patient or participant testing provide valuable insights into real-world effectiveness. For example, Beom et al. [13] tested their system on six participants, including one post-stroke patient, showing improvements in the Fugl-Meyer Assessment (FMA) and reduced spasticity. Similarly, Díez et al. [14] demonstrated enhanced motor function in six post-stroke patients. To better understand the current landscape, we categorized these systems based on mobility, VR integration, and cost. Mobility indicates the system's portability and ease of use, VR integration assesses the presence and type of virtual task, and cost reflects the estimated system's affordability - based on size, power unit type, custom materials, and materials cost. Table I summarizes these characteristics across various studies.

TABLE I: Student-Teacher System Specifications

Source	Mobility	VR	Cost
Bae et al. [11]	Low	None	High
Beom et al. [13]	Low	None	Medium
Díez et al. [14]	High	No ADL focus	High
He et al. [15]	High	No ADL focus	Medium
Kim et al. [16]	High	None	Low
Luo et al. [17]	Low	None	High
Pu & Chang [12]	Low	None	High
Ramlee & Yusoff [18]	Medium	None	Medium
Ruggiu & Rea [19]	Medium	None	Medium
STAR-eX - AM Mode	High	ADL focused	Low

As shown, the STAR-eX system stands out for its High mobility, Low cost, and ADL focused VR integration, leveraging State-of-the-Art (SotA) technologies like the Leap Motion Controller.

III. METHODOLOGY

A. STAR-eX System Components

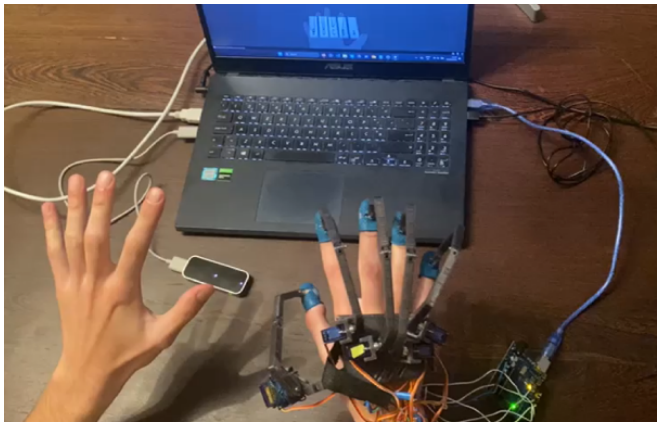

Fig. 1: Experimental Setup: To the left is the Leap Motion Controller, to the right the 21-DoF manipulator, and in the middle, the piano task being processed via Unity Game Engine.

a) Leap Motion Controller: The Leap Motion Controller captures skeletal hand data using infrared cameras and computer vision, with sub-millimeter precision. Its 140×120° field of view, 10-60 cm range, and 120 Hz tracking support real-time motion and flexible mounting[2].

b) Parallel Manipulator: The Parallel Manipulator[3] uses five micro servos controlled by an Arduino UNO to provide 5 active and 16 passive DoF, enabling versatile hand positioning. Workspace boundaries depend on the passive joints near the metacarpal region.

The passive joints influence workspace limits, particularly at the Proximal Interphalangeal (PIP) and Distal Interphalangeal (DIP) joints. Figure 2 shows fully collapsed and extended workspace boundaries, highlighting active (green) and passive (red) revolute joints.

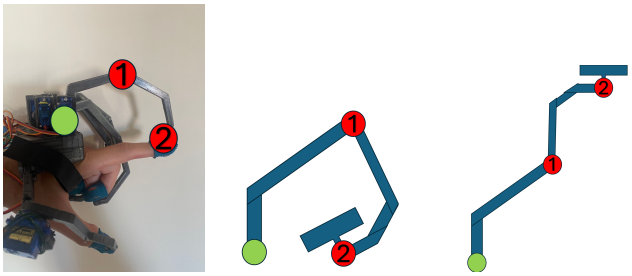

(a) Index Finger and Revolute Joints (b) Collapsed Workspace (c) Extended Workspace

Fig. 2: Active and Passive Revolute Joints

Human biomechanical constraints further limit the Range of Motion (RoM), requiring processing algorithms to ensure the manipulator does not harm users.

c) VR Interface: The VR Interface uses the LeapC[4] Unity package to interface with the motion sensor. The structured pipeline records participant data, provides feedback via animations, and uses visual cues to guide key presses [3].

d) System Cost: : The system costs approximately €168, with key components including the Leap Motion Controller (€113), Arduino UNO (€19), and five micro servos (€15). Additional expenses cover parts like thimbles, bolts, and a small circuit board.

B. Internal STAR-eX Architecture

The STAR-eX[5] system integrates a student-teacher architecture, using Finite State Machines (FSMs) and smooth trajectory guidance for data flow and servo actuation. Unity tracks user input, while an Arduino-based control system executes precise servo movements, ensuring responsive behavior. Figure 4 illustrates the architecture, showing how data flows from the VR piano task to physical actuation. An event e_i, such as a key press or release, triggers a sequence of computations and state transitions in Unity and Arduino FSMs, leading to smooth servo movements.

[2]https://www.ultraleap.com/datasheets/Leap$_{M}$otion$_{C}$ontroller$_{D}$atasheet.pdf
[3]https://github.com/BerkeleyCurtis/EECS249$_{H}$apticGlove/tree/main
[4]https://docs.ultraleap.com/api-reference/tracking-api/leapc-guide.html
[5]https://github.com/AcaAac/STAR-eX

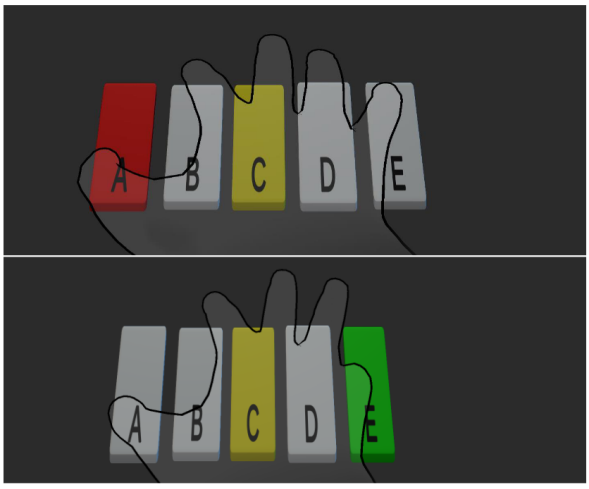

Fig. 3: Piano Key Cues - Correct, Next, Incorrect Key Press

1) Unity Finite State Machine (FSM): The Unity FSM acts as the teacher, processing VR piano task events and transmitting desired angles (θ_{d_i}) to the Arduino FSM. It monitors MCP joint angles to detect key press events. Each finger is tracked separately to minimize sensor noise and overload. When a finger's MCP angle (α_{FINGER}, where $FINGER \in \{\text{T, I, M, R, P}\}$ for thumb, index, middle, ring, and pinky, respectively) exceeds its corresponding press threshold (t_{1F}), Unity signals a key press, remaining in the "down" state until the angle falls below the release threshold (t_{2F}). The desired angle for each finger (θ_{d_i}) is updated to the current α_{FINGER} during this process.

Unity outputs the key state (*up* or *down*) and desired angle (θ_{d_i}) for the Arduino FSM to calculate smooth servo trajectories.

The event equation governing the input event type e_i is defined as follows:

$$e_i \in \{\text{up}, \text{down}\} \tag{1}$$

2) Arduino Finite State Machine (FSM): The Arduino FSM, as the student, executes commands received from Unity. It operates with separate FSMs for each finger to ensure reliable performance. Each finger's FSM goes through four primary states:

- *Idle*: No movement detected.
- *Down*: Activated on receiving key press signal.
- *Pressed*: Holds the servo at the desired angle.
- *Up*: Initiates release when the key press signal clears.

This state sequence ensures smooth, jitter-free servo movements, avoiding interference and parasitic torque effects from the fingers.

3) Smooth Trajectory Guidance: The Arduino FSM employs smooth trajectory guidance to ensure natural servo movements. Using the equations provided, intermediate angles are computed between consecutive states, and the smoothing factor (α) is applied to transition angles incrementally. This method minimizes abrupt movements and enhances stability.

The equations governing the smooth trajectory guidance are as follows:

$$\theta_t = \theta_{d_{i-1}} + \alpha \Delta\theta_{d_i}, \quad \alpha = 0.1 \tag{2}$$

$$\Delta\theta_{d_i} = \theta_{d_i} - \theta_{d_{i-1}} \tag{3}$$

Here, θ_t represents the servo's current angle, θ_{d_i} is the desired angle, and α is the smoothing factor.

The trajectory is computed as follows:

1) Calculate the angle difference ($\Delta\theta_{d_i}$) between current and desired states.
2) Apply the smoothing factor (α) to determine the incremental step.
3) Update the servo angle (θ_t) until the desired angle (θ_{d_i}) is reached.

This approach ensures responsive and precise finger movements, aligning with the VR piano task.

C. User Study

1) Overview: The experiment involved 16 healthy participants (9 males, 7 females), aged 20-55 years, conducted at Instituto Superior Técnico/University of Lisbon. All participants signed an informed consent in accordance with the 1964 Declaration of Helsinki. Fifteen participants completed three condition protocols—Active Mirror (AM), Kinesthetic (K), and Passive Mirror (P)—while Participant 0 completed only the P and K protocols.

2) Condition Training Protocols: Participants were subjected to three distinct condition training protocols, each designed to simulate different rehabilitation approaches:

a) AM - Active Mirror: The manipulator mirrors the movements performed by the teacher (left) hand, piano playing, and forces these movements onto the student (right) hand. This protocol aims to simulate RMT by combining the principles of mirror therapy with robotic assistance to enhance the rehabilitation experience.

b) K - Kinesthetic: In this protocol, the manipulator is controlled by the computer to enforce the correct key presses on the student (right) hand, regardless of the movements made by the teacher hand. This externally guided approach simulates traditional RT, where the device assists the user in completing the required tasks.

c) P - Passive Mirror: Here, the teacher (left) hand performs the piano tasks, but the manipulator is not engaged, and no movements are transmitted to the student (right) hand. This protocol represents standard MT, focusing on self-directed training without robotic intervention.

3) Experimental Design: The experiment employed a pre-test/post-test design across three training protocols (AM, K, P), each associated with five unique Discrete Sequence Progress Tasks (DSPTs). Participants completed the tasks using specific finger-to-key mappings: the thumb for *A*, the index finger for *B*, the middle finger for *C*, and the pinky finger for *E*. The ring finger (*D*) was not included due to inconsistent kinematic data from the Leap Motion Controller.

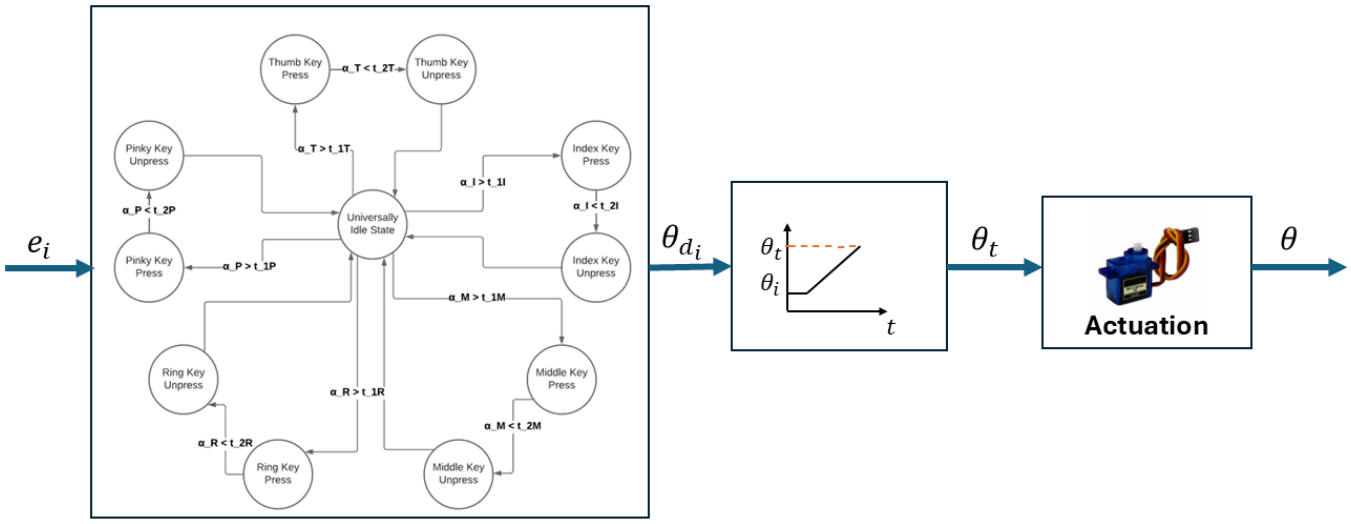

Fig. 4: Overview of the STAR-eX architecture, depicting the interaction between Unity FSM, Arduino FSM, and the smooth trajectory guidance system.

During both the pre-test and post-test phases, participants used their "student" hand to play each DSPT sequence once. The sequences used were *AECECACECABAEBECB*, *AECBAECACEB*, *CEABECABEBABCAEBC*, *ACEABACBECABCAE*, and *BEBECEABEA*. However, the key distinction lies in the post-test phase: before this phase, participants underwent a training session with their "teacher" hand. This training involved five repetitions of each DSPT using the assigned protocol (AM, K, or P). The training aimed to evaluate the effects of practice on the subsequent performance during the post-test phase.

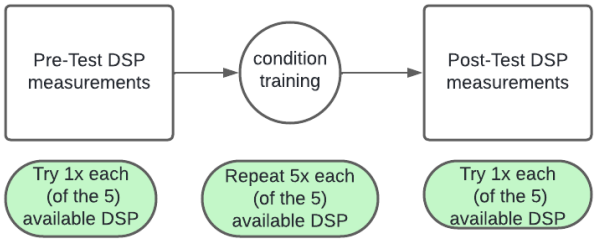

Fig. 5: Experimental Block. Each block includes three phases: Pre-Test - Participants complete each DSPT once with their student hand, without the manipulator. Condition Training - Five repetitions of each DSPT are completed using the teacher hand following the assigned protocol (AM, K, or P). Post-Test - Participants repeat each DSPT once more with their student hand, free from the manipulator. Wash-Out Intervals of 5 minutes are provided between blocks to reduce learning carry-over effects.

4) Participant Setup: Prior to beginning the experiment, participants completed the Edinburgh Handedness Inventory (EHI) questionnaire and engaged in a 5-minute warmup session. This warmup involved playing a simple *ABCE* sequence using the manipulator and motion controller integrated via the Unity engine. This familiarization ensured participants were comfortable with the device and task requirements.

5) Data Collection: Data collection focused on several metrics: the completion time for each DSPT in both the pre-test and post-test phases, the timing and number of correct and incorrect key presses, and the kinematic data (specifically MCP joint angles) for the AM and P conditions during training and test phases. Data from the ring finger were omitted due to the aforementioned issues with the Leap Motion Controller.

6) Participant Feedback: Participants completed the System Usability Scale (SUS), a ten-item questionnaire that provides a reliable measure of system usability on a scale of 0 to 100, with higher scores indicating better usability, to assess the usability of the system after completing the experiment.

D. Data Formulation

The experimental data consists of time differences, inter-key intervals, errors and kinematic data.

The average task completion time was calculated for both pre- and post-test stages to assess improvements:

$$\bar{t}_{\text{Pre;Post}} = \frac{\sum_{i=1}^{5} \text{time}(\text{DSPT}}{i)_{\text{Pre;Post}} 5(4)}$$

The Inter-Key Interval (IKI) measures the time between successive correct key presses, averaged across the five repetitions, to evaluate timing consistency:

$$\text{IKI} = t_{i+1} - t_i \tag{5}$$

Error data, including error percentage and the Error Efficiency Ratio (EER), was analyzed to assess accuracy and error reduction across the pre- and post-test stages:

$$\text{errors}_{\%} = \frac{\sum_{i=1}^{5} \text{errors}(\text{DSPT}}{i)_{\text{Pre;Post}} \sum_{i=1}^{5} \text{presses}(\text{DSPT}_i)_{\text{Pre;Post}}} (6)$$

$$EER = \frac{\sum_{i=1}^{5} \text{errors}_{\text{Pre}} - \sum_{i=1}^{5} \text{errors}_{\text{Post}}}{\sum_{i=1}^{5} \text{errors}_{\text{Pre}}} \quad (7)$$

For the kinematic analysis, we calculated the mean velocity, acceleration, and jerk of the MCP joint angles during the pre- and post-test phases across all sequences. Specifically, we determined the average (mean) velocity for each training condition and sequence during both the pre-test and post-test phases. These values were then utilized in the following formula to compute a Hand Index (HI), which provides an aggregate measure of how the training conditions influenced overall hand performance:

$$HI = \frac{\sqrt{\sum_{f \in \text{Fingers}} (\Delta \text{mean}_{(\text{Pre;Post})_f})^2}}{4} \quad (8)$$

Here, HI evaluates the variation in mean velocities across all fingers. A higher HI value indicates greater inconsistency in hand movements and suggests reduced motor control stability resulting from the training conditions.

IV. RESULTS & DISCUSSIONS

A. Time Differences

The difference of the average time taken per participant between the pre- and post-tests were calculated for each condition to determine task completion improvements.

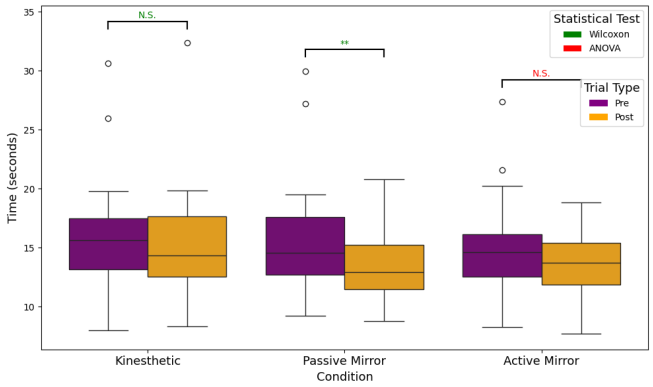

Fig. 6: Pre- vs Post-Test Average Time Difference for All Conditions. This box plot compares the average time taken between the Pre-Test and Post-Test across the (K), (P), and (AM) conditions. The (P) condition achieved significant statistical relevance with a *p-value* = 0.0076.

The P Condition showed the greatest improvement in task completion time, with the average decreasing from 15.90 to 13.39 seconds and the median from 14.57 to 12.92 seconds. Performance variability also decreased, as indicated by a reduction in standard deviation from 5.46 to 2.88 seconds..

The AM Condition saw a decrease in average time from 15.23 to 13.59 seconds and a median reduction from 14.65 to 13.74 seconds. Standard deviation dropped from 4.70 to 2.93 seconds, but the improvement was not statistically significant (p = 0.2794).

The K Condition exhibited minimal change, with the average decreasing from 16.24 to 15.52 seconds and the median from 15.62 to 14.35 seconds. Variability remained high (standard deviation: 5.44 to 5.20 seconds), and results were not statistically significant (p = 0.9799).

B. Inter-Key Interval

The Inter-Key Interval (IKI) analysis measured changes in the timing consistency between successive key presses, providing insight into participants' timing and precision.

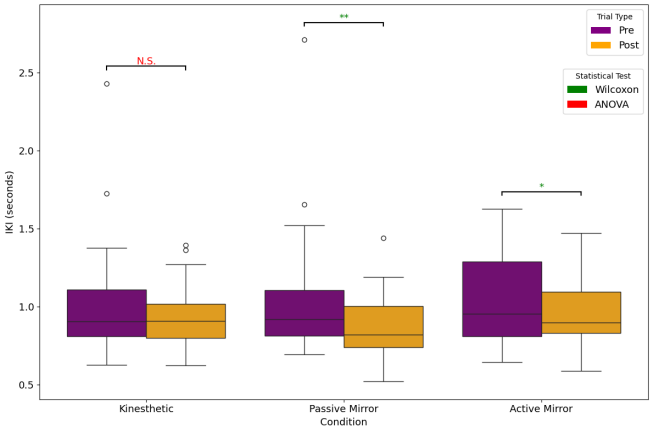

Fig. 7: Pre- vs Post-Test IKI Difference for All Conditions. This box plot compares the IKI difference between the Pre-Test and Post-Test across the three conditions: Kinesthetic (**K**), Passive Mirror (**P**), and Active Mirror (**AM**). Both the Passive Mirror and Active Mirror conditions demonstrated significant changes in IKI, with *p-values* of 2.31×10^{-4} and 0.019 (both Wilcoxon), respectively.

The P Condition showed the greatest improvement in timing consistency, with mean IKI decreasing from 1.0179 to 0.8715 seconds and median IKI from 0.9180 to 0.8195 seconds. Variability reduced significantly, as indicated by a drop in standard deviation from 0.3367 to 0.1925 seconds. This change was statistically significant (p = 0.0002).

The AM Condition showed a slight improvement, with mean IKI decreasing from 1.0454 to 0.9587 seconds and median from 0.9520 to 0.8970 seconds. Standard deviation decreased from 0.2925 to 0.2331 seconds. This result was statistically significant (p = 0.0193).

The K Condition exhibited minimal change, with mean IKI decreasing from 0.9872 to 0.9278 seconds and median IKI remaining stable (0.9045 to 0.9070 seconds). Variability showed a slight increase, but results were not statistically significant (p = 0.2329).

C. Error Data Analysis

The analysis of error data provides insights into accuracy improvements by comparing changes in error percentages

and the Error Efficiency Ratio (EER) across the pre- and post-tests.

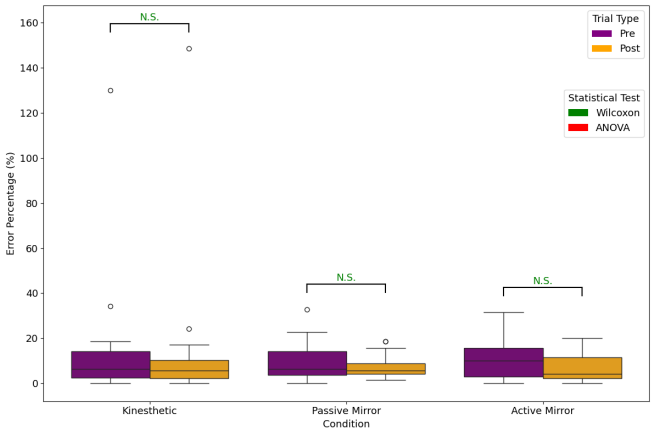

Fig. 8: Pre- vs Post-Test Error Percentage Difference for All Conditions. This box plot compares the percentage of errors increased or decreased in the Post-Test from the Pre-Test and across the three conditions: Kinesthetic (**K**), Passive Mirror (**P**), and Active Mirror (**AM**). There was no statistical relevancy in the results.

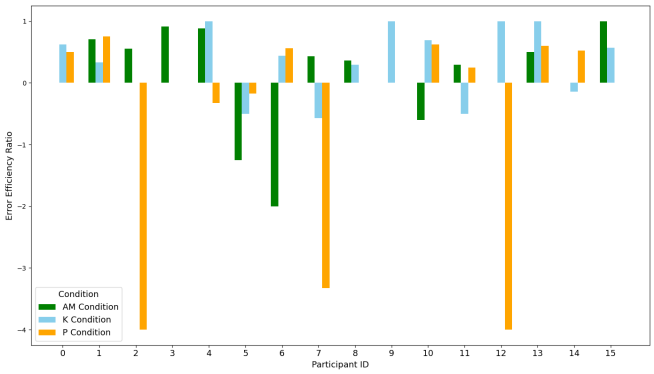

Fig. 9: Error Efficiency Ratio for - P, AM and K Conditions. $EER = 0$ means same amount of errors pre- and post-test.

In the P Condition, error percentages decreased, with the mean dropping from 10.00% to 7.77% and the median from 6.43% to 5.71%. Standard deviation reduced from 9.61% to 5.37%, indicating more consistent performance. Despite these improvements, results were not statistically significant (p = 0.3274), with 43.75% of participants reducing their EER.

The AM Condition showed notable improvements, with mean error dropping from 11.91% to 7.05% and median from 10.00% to 4.29%. Standard deviation decreased from 11.35% to 6.07%, reflecting greater accuracy and consistency. Although results were not statistically significant (p = 0.0867), 78.75% of participants had positive EERs.

The K Condition exhibited minimal changes, with mean error slightly decreasing from 16.34% to 15.71% and median from 6.43% to 5.71%. Variability increased, as standard deviation rose from 31.61% to 36.09%. Results were not statistically significant (p = 0.5619), with 62.5% of participants improving and 12.5% maintaining their EERs.

D. Kinematic Data Analysis

The kinematic data analysis examined velocity, acceleration, and jerk for various sequences in each condition. The tables below summarize the Hand Index (HI) values for each sequence under the K Condition, P Condition, and AM Condition.

When looking at every sequence's Hand Index (HI), the following values were obtained:

TABLE II: Hand Index Velocity Table for Every Sequence

Sequence	K Condition	P Condition	AM Condition
BEBECEABEA	47.28	22.01	13.94
CEABECABEBABCAEBC	14.68	16.70	29.93
ACEABACBECABCAE	46.57	35.11	32.13
AECBAECACEB	31.43	43.18	33.66
AECECACECABAEBECB	28.16	57.49	12.33

TABLE III: Hand Index Acceleration Table for Every Sequence

Sequence	K Condition	P Condition	AM Condition
BEBECEABEA	22498.50	13879.67	65046.27
CEABECABEBABCAEBC	12054.26	12746.71	35720.78
ACEABACBECABCAE	2294.62	12803.37	23100.29
AECBAECACEB	21259.09	39987.24	37302.23
AECECACECABAEBECB	21873.47	16140.94	17640.30

TABLE IV: Hand Index Jerk Table for Every Sequence

Sequence	K Condition	P Condition	AM Condition
BEBECEABEA	2983000.83	1604037.57	4734662.27
CEABECABEBABCAEBC	1501835.53	807787.39	352576.69
ACEABACBECABCAE	757060.40	1273183.53	2800062.03
AECBAECACEB	1350504.57	2167169.89	3454579.53
AECECACECABAEBECB	679343.68	1676902.19	1076054.13

This analysis reveals that the AM Condition generally exhibits lower variability in velocity compared to both the K Condition and P Condition. However, it shows higher variability in acceleration and jerk across 80% of sequences relative to the K Condition and in over 60% of sequences relative to the P Condition.

E. Active Mirror vs Kinesthetic Conditions

The AM and K conditions reveal distinct effects on motor skills. The AM Condition led to a significant reduction in task time, suggesting participants developed efficient strategies, influenced by RMT feedback. Error reduction trends were similar, though AM showed 3.75% better outcomes and more error retention than K, with three additional IKI improvements, indicating more consistent skill refinement. Kinematics showed that the AM Condition had lower velocity variability but high acceleration and jerk variability, indicating inconsistent transitions. In contrast, K Condition maintained lower variability across all measures, supporting superior motor control with stable movements.

Overall, the K Condition excelled in refining motor control, promoting precise movements. Meanwhile, AM Condition fostered better task performance and active engagement, encouraging motor skill development with a self-directed, bimanual approach inspired by RMT.

F. Active Mirror vs Passive Mirror Conditions

The comparison between the AM and P conditions showed both improved task completion time, but P achieved a greater reduction (2.5 seconds) with statistical significance (*p-value* = 0.0076), suggesting rapid adaptation likely from MT. In error reduction, P showed slightly lower improvement but higher retention than AM. For IKI, 14 P participants improved ($p\text{-}value = 2.31e-04$) versus 10 in AM ($p\text{-}value = 0.019$). Kinematics supported P, showing lower variability in acceleration and jerk compared to AM, which exhibited high variability in 60-80% of sequences. This stability in P suggests classical MT offers a more consistent motor control foundation. The predominantly right-handed participants in P may have naturally leveraged their dominant side, enhancing performance, though future studies with more diverse samples could clarify STAR-eX and RMT benefits.

V. CONCLUSIONS

This study evaluated the efficacy of STAR-eX's RMT in comparison to its RT and MT modes for enhancing motor skill and control. Current results suggest that the RMT mode can lead to greater motor skill enhancement compared to the RT. However, in terms of motor control refinement, STAR-eX's MT mode demonstrated superior skill acquisition and control improvement, benefiting from dominant-hand reliance and minimal device constraints.

Several limitations were identified in the study. The sample of right-handed participants limited the generalizability of the findings, particularly regarding kinematic data. Sensor adaptation issues, notably with the ring finger's MCP joint, impacted data quality, highlighting the need for better finger tracking and calibration. Biomechanical differences between participants emphasized the importance of personalized FSM calibrations. Additionally, hardware limitations, such as single-key presses, restricted task complexity. Future work should address these limitations by incorporating Bluetooth connectivity to enhance task versatility and the system's usability in therapeutic contexts.

REFERENCES

[1] Hatem A. Wafa, Charles D.A. Wolfe, Eva Emmett, Gregory A. Roth, Catherine O. Johnson, and Yanzhong Wang, "Burden of Stroke in Europe," *Stroke*, vol. 51, no. 8, pp. 2418–2427, 2020. doi: 10.1161/STROKEAHA.120.029606.

[2] Gunilla E. Frykberg and Rajul Vasa, "Neuroplasticity in action post-stroke: Challenges for physiotherapists," *European Journal of Physiotherapy*, vol. 17, no. 2, pp. 56–65, 2015. doi: 10.3109/21679169.2015.1039575.

[3] Nedim Ongun and Attila Oguzhanoglu, "Comparison of the Nerve Conduction Parameters in Proximally and Distally Located Muscles Innervated by the Bundles of Median and Ulnar Nerves," *Medical Principles and Practice*, vol. 25, no. 5, pp. 466–471, 2016. doi: 10.1159/000447742.

[4] Elger Abrahamse, Marit Ruitenberg, Elian De Kleine, and Willem B. Verwey, "Control of automated behavior: insights from the discrete sequence production task," *Frontiers in Human Neuroscience*, vol. 7, 2013. doi: 10.3389/fnhum.2013.00082.

[5] Mónica Cameirão, Sergi Bermúdez i Badia, Esther Duarte, and Paul Verschure, "Virtual reality based rehabilitation speeds up functional recovery of the upper extremities after stroke: A randomized controlled pilot study in the acute phase of stroke using the Rehabilitation Gaming System," *Restorative Neurology and Neuroscience*, vol. 29, pp. 287–298, 2011. doi: 10.3233/RNN-2011-0599.

[6] Gerard G. Fluet, Devraj Roy, Roberto Llorens, Sergi Bermúdez i Badia, and Judith E. Deutsch, "Basis and Clinical Evidence of Virtual Reality-Based Rehabilitation of Sensorimotor Impairments After Stroke," in *Neurorehabilitation Technology*, Springer International Publishing, Cham, 2022, pp. 429–466. doi: 10.1007/978-3-031-08995-4_20.

[7] Priscilla G. Wittkopf and Mark I. Johnson, "Mirror therapy: A potential intervention for pain management," *Revista da Associação Médica Brasileira*, vol. 63, no. 11, pp. 1000–1005, 2017. doi: 10.1590/1806-9282.63.11.1000.

[8] Mareike Schrader, Annette Sterr, Robyn Kettlitz, Anika Wohlmeiner, Rudiger Buschfort, Christian Dohle, and Stephan Bamborschke, "The effect of mirror therapy can be improved by simultaneous robotic assistance," *Restorative Neurology and Neuroscience*, vol. 40, no. 3, pp. 185–194, 2022. doi: 10.3233/RNN-221263.

[9] Md Rasedul Islam, Christopher Spiewak, Mohammad Rahman, and Raouf Fareh, "A Brief Review on Robotic Exoskeletons for Upper Extremity Rehabilitation to Find the Gap between Research Prototype and Commercial Type," *Advances in Robotics & Automation*, vol. 6, 2017. doi: 10.4172/2168-9695.1000177.

[10] Angelo Basteris, Sharon Nijenhuis, Arno Stienen, Jaap Buurke, Gerdienke Prange, and Farshid Amirabdollahian, "Training modalities in robot-mediated upper limb rehabilitation in stroke: A framework for classification based on a systematic review," *Journal of Neuroengineering and Rehabilitation*, vol. 11, no. 111, 2014. doi: 10.1186/1743-0003-11-111.

[11] Ju-Hwan Bae, Young-Min Kim, and Inhyuk Moon, "Wearable hand rehabilitation robot capable of hand function assistance in stroke survivors," in *2012 4th IEEE RAS & EMBS International Conference on Biomedical Robotics and Biomechatronics (BioRob)*, 2012, pp. 1482–1487. doi: 10.1109/BioRob.2012.6290736.

[12] Shu-Wei Pu and Jen-Yuan Chang, "Robotic hand system design for mirror therapy rehabilitation after stroke," *Microsyst. Technol.*, vol. 26, no. 1, pp. 111–119, 2020. doi: 10.1007/s00542-019-04483-3.

[13] Jaewon Beom, Sukgyu Koh, Hyung Seok Nam, Wonshik Kim, Yoon Kim, Han Gil Seo, Byung-Mo Oh, Sun Chung, and Sungwan Kim, "Robotic Mirror Therapy System for Functional Recovery of Hemiplegic Arms," *Journal of Visualized Experiments*, vol. 2016, 2016. doi: 10.3791/54521.

[14] Jorge Díez, Andrea Blanco, José M. Catalán, Francisco Badesa, Luis Lledo, and Nicolas Garcia, "Hand exoskeleton for rehabilitation therapies with integrated optical force sensor," *Advances in Mechanical Engineering*, vol. 10, pp. 168781401775388, 2018. doi: 10.1177/1687814017753881.

[15] Bo He, Min Li, and Guoying He, "Hand Rehabilitation Modes Combining Exoskeleton-Assisted Training with Tactile Feedback for Hemiplegia Patients: A Preliminary Study," in *Neurorehabilitation Technology*, Springer, Cham, 2022, pp. 661–669. doi: 10.1007/978-3-031-13835-5_60.

[16] Dong Kim, Kun-Do Lee, Thomas Bulea, and Hyung-Soon Park, "Increasing Motor Cortex Activation During Grasping Via Novel Robotic Mirror Hand Therapy: A Pilot fNIRS Study," 2021. doi: 10.21203/rs.3.rs-810023/v1.

[17] Haiyi Luo, Zhenyu Sun, Xiaobei Jing, Bairui Shu, Shixiong Chen, Xu Yong, and Hiroshi Yokoi, "Development and evaluation of a hand exoskeleton for finger rehabilitation," in *2022 IEEE International Conference on Robotics and Biomimetics (ROBIO)*, 2022, pp. 1673–1678. doi: 10.1109/ROBIO55434.2022.10011966.

[18] Mohd Ramlee and Hazlina Yusoff, "Design and development of gripping assistive device for post-Stroke rehabilitation," in *2017 IEEE International Conference on Signal and Image Processing Applications (ICSIMA)*, 2017, pp. 1–5. doi: 10.1109/ICSIMA.2017.8312030.

[19] Maurizio Ruggiu and Pierluigi Rea, "Development of a Mechatronic System for the Mirror Therapy," *Actuators*, vol. 11, no. 1, pp. 14, 2022. doi: 10.3390/act11010014.